# Measurement-based Delay Spread Analysis of Wideband Massive MIMO System at 3.5 GHz

Chongpeng Xu, Jianhua Zhang, Qingfang Zheng, Hao Yu, Lei Tian
Key Lab of Universal Wireless Communications, Ministry of Education
Beijing University of Posts and Telecommunications, P. O. Box 92, Beijing 100876, China
Email: xuchongpeng@bupt.edu.cn

***Abstract*—Massive multiple-input multiple-output (MIMO) ultra-wideband channel plays an important role in studying the fifth generation (5G) mobile communication system. The measurement is carried out in outdoorto-indoor (O2I) scene non-line of sight (NLoS). The frequency is 3.5 GHz and bandwidth is 100 MHz and 200 MHz respectively. Through the analysis of measurement data, two problems are explored in this parper. One is the method used to evaluate delay spread in such a large number of sub-channel system. Another is the effect of the transmission bandwidth and antenna number. The results reflect that array positions and measurement environments have various influences on delay spread. In addition, contrasting the results of different bandwidth, it clearly indicates that the delay spread of 100 MHz is greater.**

## I. Introduction

With the development of smart phones and mobile applications, mobile communications have experienced explosive growth. The mobile traffic is predicted to grow more than 1000 times in the next 10 years [1]. Many theoretical studies combining with the measurement or simulation data report very promising system performance, see [2], [3]. In [2], the author analyze the propagation characteristics in an outdoor scenario with a physically large array, and concludes that large scale fading and a varying angular power spectrum will be observed over the array. The performance of transmit antenna selection in the measured massive multiple-input multiple-output (MIMO) channels was studied in [3], showing that the compact cylindrical array achieves better performance than the physically large linear array.

Most of studies of delay spread stay in MIMO system [4]–[6]. [4], [5] summarized the delay spread characteristics and capacity performance of a 2 TX and 2 RX wideband MIMO channel system. [6] present the root mean square (RMS) delay spreads and their probability distribution, roughly follows Gaussian distribution, based on the wideband MIMO measurement data. [7] analyzed the effects of different linear precoding schemes based on measured data from a massive MIMO channel system with 128 antennas at the base station and 36 users. The results show that the compact cylindrical array achieves better performance than the physically large linear array. Our study on delay spread in wideband massive MIMO system, comparing two bandwidth of 100 MHz and 200 MHz, can be the first time. The rationality of the virtual measurement was proved in [8], the power delay profile (PDP) calculated from combined channel impulse response (CIR) and CIR collected from the measurement campaigns can fit well.

In this paper, the delay spread characteristics of the wideband massive MIMO channel are presented.

## II. Measurement Description

The measurement of massive MIMO channel was performed on the campus of Beijing University of Posts and Telecommunications (BUPT), China, utilizing the Elektrobit Propsound sounder at a carrier frequency of 3.5 GHz and the signal bandwidth of 100 MHz and 200 MHz respectively. A 32-element uniform patch array (UPA) and a 16-element omnidirectional array (ODA) are selected to conduct the measurement. Fig. 1 shows the dual-polarized UPA with 32 antenna elements at the transmitting terminal. We shift the position of transmitting antenna (including the horizontal and vertical positions) and a virtual massive MIMO antenna array is obtained after the measured data processing. Fig. 2 illustrates the schematic diagram of shifting the position of a single 32-element UPA to form a larger antenna array in a short time, and the distance of each single element is half-wavelength.

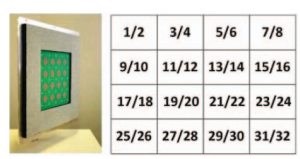


Fig. 1. Layout and schematic of antenna array at TX side.

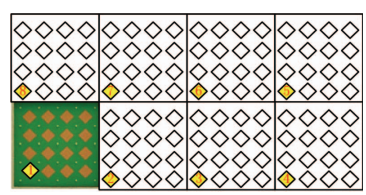

Fig. 2. Virtual antenna array positions.

During the measurement, TX is located on the top of a lower building, while RX is at 4th floor in a higher building. Layout of the 4th floor is illustrated in Fig. 3.

## III. Data Processing Methods

### A. Power Delay Profile

The measured CIR collected by the sliding correlation detector at time $t_n$ can be modeled as $h(\tau_l, t_n), l = 1, \cdots, N$,

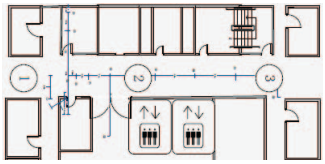

Fig. 3. Layout of the 4th floor.

where $\tau_l$ indicates the delay of the $l$th sample in the delay domain. $N$ is the sampling length of a CIR snapshot at time $t_n$. The PDP corresponding to the CIR at time $t_n$ can be calculated by

$$P(\tau_l, t_n) = \|h(\tau_l, t_n)\|^2, l = 1, \cdots, N \tag{1}$$

where $\|\cdot\|$ indicates 2-norm operation.

A typical PDP result of a certain sub-channel at a certain measurement spot is shown in Fig. 4. The threshold is set to $(X_n)$ 10 dB larger than the noise level. The sub-path set of the CIR can be further defined by

$$A_n = \{h(\tau_l, t_n) \mid P(\tau_l, t_n) > X_n, l = 1, \cdots, N\}, \tag{2}$$

where $X_n$ is the threshold at time $t_n$.

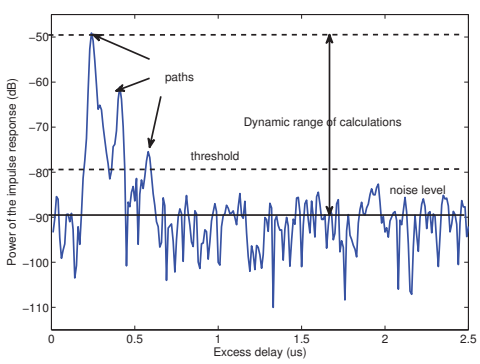


Fig. 4. Power Delay Profile.

### B. Delay

The RMS delay is defined as the root mean square of second central moment of the PDP [9]. So the RMS delay sample of a certain CIR can be simply calculated by

$$\sigma_\tau(t_n) = \sqrt{\overline{\tau^2(t_n)} - \overline{\tau(t_n)}^2}, \tag{3}$$

where $\overline{\tau^2(t_n)}$ and $\overline{\tau(t_n)}^2$ can be calculated by

$$\overline{\tau^2(t_n)} = \frac{\sum_{\tau_l \in U_n} P(\tau_l, t_n)\tau_l^2}{\sum_{\tau_l \in U_n} P(\tau_l, t_n)}, \tag{4}$$

and

$$\overline{\tau(t_n)} = \frac{\sum_{\tau_l \in U_n} P(\tau_l, t_n)\tau_l}{\sum_{\tau_l \in U_n} P(\tau_l, t_n)}, \tag{5}$$

where

$$U_n = \{\tau_l \mid h(\tau_l, t_n) \in A_n, l = 1, \cdots, N\}. \tag{6}$$

These delays of $\tau_l$ are measured relative to the first detectable signal arriving at the receiver at $\tau_0 = 0$.

TABLE I
THE FITTING PARAMETERS OF 8 TX ANTENNA ELEMENTS COMPARISON

| TX position | $\mu(log_{10}(s))$ | $\mu(ns)$ | $\sigma(log_{10}(s))$ |
|---|---|---|---|
| 1 | -7.01 | 98 | 0.1297 |
| 2 | -7.02 | 95 | 0.1355 |
| 3 | -7.00 | 100 | 0.1293 |
| 4 | -6.92 | 120 | 0.1078 |
| 5 | -6.96 | 110 | 0.0955 |
| 6 | -6.92 | 120 | 0.1127 |
| 7 | -6.92 | 120 | 0.1135 |
| 8 | -6.94 | 115 | 0.0861 |

## IV. RESULTS AND ANALYSIS

In our measurement, there are $256 \times 16 = 4096$ multipaths intensity profiles in a snapshot. As there are so many multipaths, several antenna elements are picked from TX. The TX antenna is the left bottom antenna element 25# $-$26# on UPA, and the RX is the whole 16 antenna elements on ODA. There are $2 \times 16 = 32$ subchannels considered on one position, and there are 8 positions as shown in Fig. 2.

Fig. 5 shows the histogram of RMS delay spread($log_{10}(s)$) distribution at TX position number 1 with bandwidth of 200 MHz. It is fitted well by the Gaussian distribution.

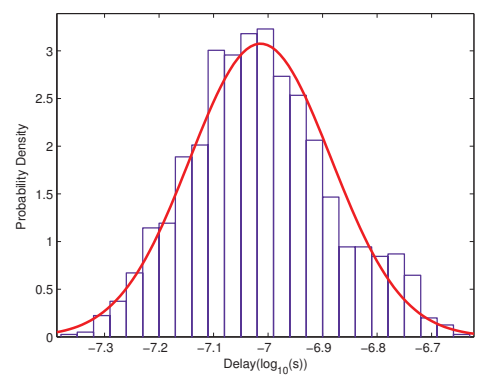


Fig. 5. PDF of RMS delay spread at TX position number 1.

The situation of other TX positions are close to the number 1 position, fitting well by Normal distribution. The fitting parameters $\mu(log_{10}(s))$ and $\sigma(log_{10}(s))$ of the RMS delay spread are all listed in Table I. On comparing the statistics parameters, it obviously shows that the TX array positions have impact on the RMS delay spread in our measurement. The maximum of $\mu(ns)$ is about 120, however the minimum is 95. The dispersion can be measured by $(\mu_{max} - \mu_{min})/\bar{\mu}$, which is 0.2278.

Fig. 6 shows the cumulative distribution functions (CDF) of the RMS delay spread at measurement spot 1 with the bandwidth of 100 MHz. With the increasing of the number of antenna elements, the discrepancy of RMS delay between each case is tending to reduce. As we can see in the figure of amplification, the four smoothing curves can fitting log-normal well, and the curve of case 3 is very close to the curve of case 4, while both have some of interval to the curves of case 2 and case 1. That means the RMS delay spread obey log-normal distribution ,and the distribution tends to be stable when the number of antenna elements is bigger enough. 128 antenna

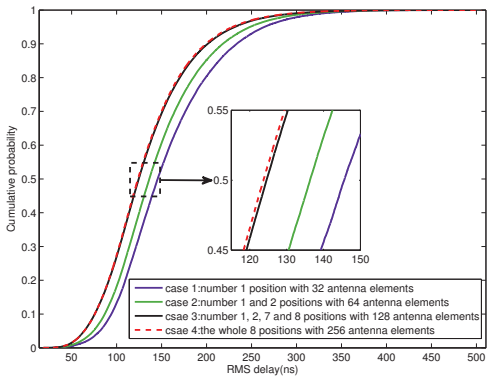


Fig. 6. CDF of RMS delay spread with different number of antenna elements.

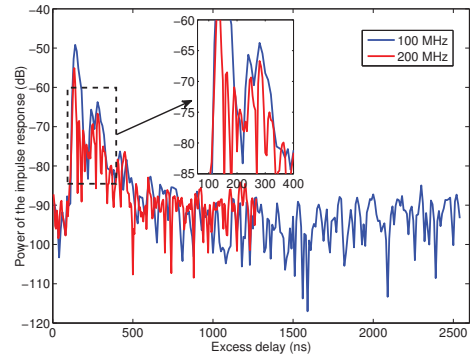


Fig. 7. Comparison of PDP between 100 MHz and 200 MHz.

TABLE II
THE FITTING PARAMETERS OF 100 MHZ AND 200 MHZ.

| spot | | 100 MHz | | 200 MHz | |
|---|---|---|---|---|---|
| | | $\mu(log_{10}(s))$ | $\sigma(log_{10}(s))$ | $\mu(log_{10}(s))$ | $\sigma(log_{10}(s))$ |
| 4th floor | 1 | -6.79 | 0.1463 | -6.93 | 0.1165 |
| | 2 | -6.80 | 0.1549 | -6.99 | 0.1215 |
| | 3 | -6.72 | 0.1478 | -6.92 | 0.0963 |

elements can be a rational choice, maybe less. But we can't come to conclusion that more antenna elements cause smaller RMS delay spread, as the result of the effect of TX positions in the big size antenna discussed above.

Ignoring differences among the sub-channels, the RMS delay spread ($log_{10}(s)$) of the whole sub-channels results can fit the Normal distribution well. Table II shows the fitting parameters $\mu(log_{10}(s))$ and $\sigma(log_{10}(s))$ of the RMS delay spread at all measurement spots. Measurement results from bandwidth of 100 MHz are greater at all measurement spots, both mean value and variance of Normal-fit. The RMS delay spread is $158 \sim 191ns$ with the dispersion of 0.1937 in 100 MHz. The result of 200 MHz is $102 \sim 120ns$ and the dispersion is 0.1592. The dispersion reflects the different degree among antenna positions, and thus it can be an important parameter for describing delay spread measurement environment. The smaller dispersion is, the more stable delay spread distribution is.

Fig. 7 shows the difference of PDP in one snapshot between 100 MHz and 200 MHz at position number 1. It can easily find a finer resolution appeared at 200 MHz in the figure of amplification. Therefore, the RMS delay spread is smaller at 200 MHz in this snapshot, as the result of more delay paths and weaker power.

## V. CONCLUSION

This paper analyzed the RMS delay spread (DS) and their probability distribution on the basis of the wideband massive MIMO channel measurement in O2I scenario at 3.5 GHz with 100 MHz and 200 MHz bandwidth respectively. The results indicate that the empirical distribution of the RMS DS are fitted well by Gaussian distribution. This method can be easily applied to large scale antenna, considering all sub-channels directly. Futhermore, the mean and variance of RMS delay spreads depend on the antenna array, practical environment and transmission bandwidth. There is a not weak impact on RMS delay spread among the antenna elements and antenna array positions, and thus the author introduces the parameter of dispersion. Besides, the larger bandwidth has smaller delay spread obviously. As the bandwidth and the size of antenna increasing, the traditional method will be inefficient.

## ACKNOWLEDGMENT

This research is supported in part by National Science and Technology Major Project of the Ministry of Science and Technology (2015ZX03001034), and in part by National Natural Science Foundation of China (61322110). This research is also supported by Huawei Technologies Co., Ltd.

## REFERENCES

[1] J. Wu, S. Rangan, and H. Zhang, *Green communications: theoretical fundamentals, algorithms and applications*. CRC Press, 2012.

[2] S. Payami and F. Tufvesson, "Channel measurements and analysis for very large array systems at 2.6 ghz," in *Antennas and Propagation (EUCAP), 2012 6th European Conference on*. IEEE, 2012, pp. 433–437.

[3] X. Gao, O. Edfors, J. Liu, and F. Tufvesson, "Antenna selection in measured massive mimo channels using convex optimization," in *Globecom Workshops (GC Wkshps), 2013 IEEE*. IEEE, 2013, pp. 129–134.

[4] J. F. Kepler, T. P. Krauss, and S. Mukthavaram, "Delay spread measurements on a wideband mimo channel at 3.7 ghz," in *Vehicular Technology Conference, 2002. Proceedings. VTC 2002-Fall. 2002 IEEE 56th*, vol. 4. IEEE, 2002, pp. 2498–2502.

[5] H. Bölcskei, D. Gesbert, and A. J. Paulraj, "On the capacity of ofdm-based spatial multiplexing systems," *Communications, IEEE Transactions on*, vol. 50, no. 2, pp. 225–234, 2002.

[6] Y. L. Yang, Z. Zhong, and G. Xu, "Delay spread characteristics of wideband mimo channels based on outdoor non-line-of-sight measurements," in *Global Telecommunications Conference, 2007. GLOBECOM'07. IEEE*. IEEE, 2007, pp. 3745–3749.

[7] S. Payami and F. Tufvesson, "Delay spread properties in a measured massive mimo system at 2.6 ghz," in *Personal Indoor and Mobile Radio Communications (PIMRC), 2013 IEEE 24th International Symposium on*. IEEE, 2013, pp. 53–57.

[8] H. Yu, J. Zhang, Q. Zheng, Z. Zheng, L. Tian, and Y. Wu, "The rationality analysis of masssive mimo virtual measurement at 3.5 ghz," *2016 Workshop, IEEE International(ICCC Workshop)*,in press.

[9] T. S. Rappaport *et al.*, *Wireless communications: principles and practice*. Prentice Hall PTR New Jersey, 1996, vol. 2.